INDERSCIENCE PUBLISHERS
Linking academia, business and industry through research

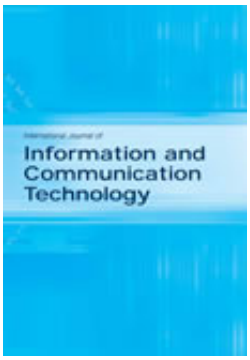

International Journal of Information and Communication Technology

ISSN online: 1741-8070 - ISSN print: 1466-6642
https://www.inderscience.com/ijict

Prediction method of battery remaining life based on CEEMDAN-RF-SED-LSTM neural network

Hanping Pan, Wenjian Feng, Jiaqi Ge, Jijun Zhang

Article History:

Received:	11 December 2023
Last revised:	04 March 2024
Accepted:	11 May 2024
Published online:	22 November 2024

Prediction method of battery remaining life based on CEEMDAN-RF-SED-LSTM neural network

Hanping Pan, Wenjian Feng, Jiaqi Ge and Jijun Zhang*

College of Automotive and Information Engineering,
Guangxi Eco-Engineering Vocational &Technical College,
Liuzhou 545004, Guangxi, China
Email: 15878292827@163.com
Email: fwjian@163.com
Email: gjq123456@163.com
Email: zhang.jijun@163.com
*Corresponding author

Abstract: In order to ensure the reliability and safety of electric vehicles, a CEEMDAN-RF-SED-LSTM method for lithium ion power battery system is proposed. Taking the time interval of equal voltage charging as the indirect health factor, taking into account the influence of external interference and capacity regeneration phenomenon, the degradation trend of battery is obtained by variational mode decomposition (VMD). The improved recurrent neural network model – short and long time series (LSTM) is used to obtain the residual life prediction. Finally, the established model is compared with FNN, CNN, LSTM and other neural networks, which gives full play to the characteristics of SCN such as strong autonomy, fast convergence speed and low network cost. The performance of this method is tested with NASA dataset as the research object. The experimental results show that CEEMDAN-RF-SED-LSTM model performs well in predicting RUL of batteries, and the prediction results have lower errors than that of a single model.

Keywords: lithium ion battery; life prediction; configure the network randomly; incremental learning.

Reference to this paper should be made as follows: Pan, H., Feng, W., Ge, J. and Zhang, J. (2024) 'Prediction method of battery remaining life based on CEEMDAN-RF-SED-LSTM neural network', *Int. J. Information and Communication Technology*, Vol. 25, No. 9, pp.1–21.

Biographical notes: Hanping Pan is a Lecturer at Guangxi University of Technology (undergraduate) and obtained his Bachelor of Engineering degree. He is currently engaged in the teaching of ecological engineering maintenance in the College of Automotive and Information Engineering, Guangxi Vocational and Technical College.

Wenjian Feng is a Professor and Senior Engineer and is mainly engaged in the research of big data technology and algorithm application.

Jiaqi Ge is a Lecturer and obtained his Bachelor's degree in Engineering from Guangxi University of Science and Technology (undergraduate). He is currently teaching in the Automotive Maintenance major at the School of Automotive and Information Engineering, Guangxi Vocational and Technical College of Ecological Engineering. His main research areas include new energy vehicle technology and intelligent connected vehicle technology.

Jijun Zhang has a Master's degree from Guilin University of Electronic Technology. He is a Lecturer at School of Automotive and Information Engineering, Guangxi Ecological Engineering Vocational and Technical College. His main research fields are new energy vehicle technology, automobile manufacturing and test technology.

1 Introduction

Lithium ion batteries are widely used in electric vehicles, energy storage systems and consumer electronics due to their long cycle life, high energy density and low cost (Zhu et al., 2022; Liao and Köttig, 2014). The lithium ion battery will cause the loss of active lithium and active materials after a long-term charge and discharge cycle, resulting in the capacity decline and energy decay of the lithium ion battery, which will shorten the remaining useful life (RUL) of the battery (Zong et al., 2022; Wang and Di, 2022). RUL prediction of lithium-ion battery is the basis for realising the maintenance of power battery system, and is of great significance for ensuring the safe and reliable operation of vehicles. The capacity and internal resistance are used as characteristic inputs to characterise the health status of the battery (Sulzer et al., 2021) It is difficult to measure capacity and internal resistance online through simple sensors. The current, voltage and temperature directly collected by the sensor are used as characteristic factors to predict the remaining life of the battery. The battery charging mode is usually constant current and constant voltage charging, which is relatively stable. Some studies show that with the aging of lithium-ion batteries, the time when the charging voltage rises to the upper limit of cut-off voltage gradually decreases (Shen et al., 2019). The charging voltage curve is used as the characteristic factor of the battery to predict the remaining life of the battery. In the actual work of the battery system, it is difficult to obtain a complete charging curve, such as the large-capacity electric bus battery system, the shallow-charged and shallow-discharged redundant satellite battery system, etc. The battery degradation process is characterised by the constant voltage charging time as the characteristic factor.

The biggest advantage of the data-driven prediction algorithm is that it does not need to know the exact model of the battery, but only needs a certain amount of degraded data to complete. Therefore, the data-driven battery RUL prediction method is more popular and widely used, and gradually becomes the mainstream method of battery life prediction (Lv et al., 2022; Yu et al., 2022). The data-driven battery RUL prediction methods mainly include artificial neural network, support vector machine, support vector regression, particle filter, etc. The artificial neural network is designed to simulate the operation of the human brain nervous system, and it shines brilliantly in the battery life prediction problem because of its strong nonlinear processing ability, adaptability and self-learning ability (Zhang et al., 2022). However, the artificial neural network brings slow training and excessive resource consumption Problems such as weak generalisation

are also slowly emerging in the process of use, which has become a difficult point hindering its development in the direction of lithium ion battery life prediction. Fortunately, the emergence of incremental learning has gradually solved these problems.

The deep neural network can be used to solve the above problems. The deep neural network (DNN) is constructed by using multiple nonlinear transformations to extract complex feature information from the input data. In recent years, several DNN-based SOC estimation methods have been proposed. In literature (Muenzel et al., 2015), the SOC estimator was constructed using the multi-layered perceptron (MLP) network and trained using the signals measured at different ambient temperatures. The results show that the trained model can reduce the estimation error of SOC. On the basis of this research, considering the advantages of long short-term memory (LSTM) in capturing time information in time series data, the literature; Ou et al., 2021) developed a SOC estimator based on LSTM to further improve the estimation accuracy, and achieved good results. As another variant of the recurrent neural network (RNN), the gated recurrent unit (GRU) neural network has also been applied to SOC estimation. Angenendt et al. (2016), and Zhang et al. (2021) introduced GRU structure into RNN network to improve the modelling ability of lithium ion battery nonlinear behaviour, and constructed two models using current and voltage signals as input to estimate SOC. However, the above documents do not consider the SOC estimation of lithium-ion batteries under variable operating conditions and will reduce the accuracy of SOC estimation under long time series signals. The above method considers the time series characteristics of lithium-ion battery data, and uses LSTM, BiLSTM and 1D CNN-LSTM to analyse lithium-ion battery data respectively. This paper combines the advantages of the above methods, uses 1D CNN to mine the deep features of lithium-ion battery data, and combines BiLSTM bidirectional (past to future and future to past) analysis feature sequence, and proposes 1D CNN-BiLSTM (Mansouri et al., 2017) hybrid neural network to realise RUL prediction of lithium-ion battery. This algorithm has the following innovations:

1 LSTM has good prediction performance, but the limitation of the above methods is that the network model parameters of LSTM need to be randomly set by human experience, and the selection of different parameters training will directly affect the network model structure and prediction accuracy. Therefore, this paper proposes a method of using whale optimisation algorithm (WOA) to optimise the super parameters of LSTM network, which makes the established lithium battery residual service life model have better prediction effect and stability. Finally, select NASA public dataset to compare WOALSTM with standard LSTM algorithm, Elman algorithm and PSO-LSTM algorithm to verify the effectiveness of the proposed model.

2 BiLSTM has rich time series analysis capabilities. Based on the forward LSTM analysis of input sequence, BiLSTM combines the reverse LSTM to carry out bidirectional processing of data to enhance the prediction accuracy of neural network.

3 LSTM and GRU introduced a simple encoder-decoder mechanism to better learn the global time characteristics and remote dependencies of sequence data. The validity of the model was verified by using the public dataset of lithium ion batteries from NASA. The experimental results show that CEEMDAN-RF-SED-LSTM performs well in the RUL prediction of batteries, and the prediction results of the combined model with RF (Wang, 2021) and SED have higher accuracy.

2 Method and principle

2.1 A.SOC estimation model of lithium ion battery based on EMD-GRU

Based on the previous introduction of EMD and GRU algorithms, an estimation method of SOC based on EMD-GRU lithium-ion battery (Duan, 2021) is proposed, as shown in Figure 1. This method uses EMD algorithm to decompose the battery current signal, decompose the current into several current sub-sequences, and then combine the battery voltage and battery temperature fluctuations as the input of GRU neural network. After passing through the full connection layer network, the battery SOC is used as the output. The existing data are trained to obtain the model parameters. New current subsequences, voltage and temperature are introduced as network inputs to predict the SOC of the network.

Figure 1 SOC estimation method of EMD-GRU lithium-ion battery (see online version for colours)

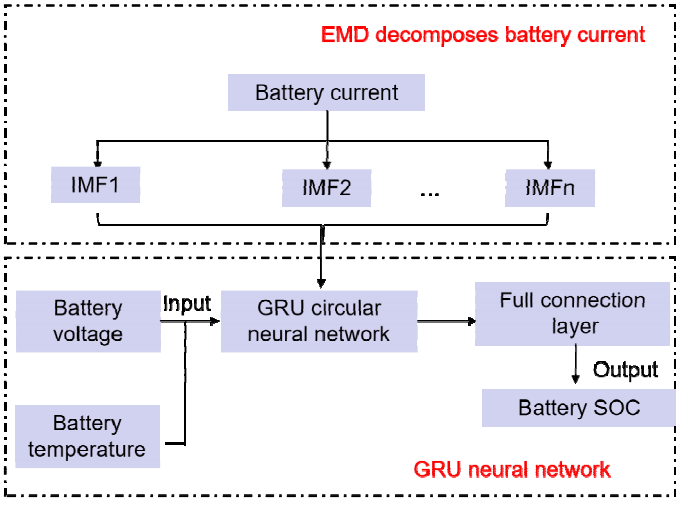

The specific steps of SOC (Dufo-López et al., 2014) estimation of EMD-GRU lithium-ion battery are as follows:

1 Data pre-processing. The accuracy of data determines the accuracy of the network model, collecting current, voltage and temperature $x_k = [I_k, V_k, T_k]$ and SOC data $y_k = \{SOC_k\}$, complete the correction of errors and missing data, and divide the training set and test set.

2 Empirical mode decomposition. Use EMD to transmit current signal I_k. Divided into sub-current sequence set $\{I_{1k}, I_{2k}, \ldots, I_{jk}\}$. In view of the large difference in the numerical units of the decomposed current sequence, the min-max normalised current subsequence set is used to scale the value to 0~1.

$$I_{ik}^{*} = \frac{I_{ik} - \min\left(I_{ik}\right)}{\max\left(I_{ik}\right) - \min\left(I_{ik}\right)} i = 1, 2, \ldots, j \tag{1}$$

Among, I_{ik}^{*} is the normalised current subsequence set.

3 Time series prediction of GRU model (Xiong et al., 2018). The GRU-based lithium ion battery SOC estimation model is established using the training set data. By setting the network structure and parameters, Adam is used as the network training optimisation algorithm, ReLU is used as the network activation function, and the mean square error (MSE) function is used as the optimisation objective function, and then the optimal SOC estimation model parameters are obtained through training (Yang, 2021).

4 Model evaluation. The test set is used as the input of the GRU model to obtain the estimated SOC value, and then the accuracy of the model is measured by the error of the predicted value and the actual value. The mean absolute error (MAE), MSE, and root mean square error (RMSE) are selected. The calculation formulas are:

$$MAE = \frac{1}{n}\sum_{i=1}^{n} | \hat{y}_i - y_i | \tag{2}$$

$$MSE = \frac{1}{n}\sum_{i=1}^{n} \left(\hat{y}_i - y_i \right)^2 | \tag{3}$$

$$RMSE = \sqrt{\frac{1}{n}\sum_{i=1}^{n} \left(\hat{y}_i - y_i \right)^2 |} \tag{4}$$

Among, $\hat{y}_i$ for no *i* predicted values; is the actual value of; Is the forecast quantity.

2.2 Based on dropout_ remaining of MC LSTM

2.2.1 Life prediction model

As a new time series prediction method, the long and short time series (LSTM) neural network overcomes the phenomenon of gradient explosion and gradient disappearance of the traditional cyclic neural network. The LSTM neural unit is used to replace the traditional cycle time network unit. LSTM neural network has long-term memory ability. LSTM neural unit mainly includes forgetting gate, output gate and input gate. Its formula is as follows.

$$i_t = \sigma \left[\omega_{xi} x_t + \omega_{hi} x_{t-1} + b_i \right] \tag{6}$$

$$f_t = \sigma \left[\omega_{xf} x_t + \omega_{hf} x_{t-1} + b_f \right] \tag{7}$$

$$o_t = \sigma \left[\omega_{xo} x_t + \omega_{ho} x_{t-1} + b_o \right] \tag{8}$$

$$c_t = f_t c_{t-1} + \tanh \left(\omega_{xc} x_t + \omega_{hc} h_{t-1} + b_c \right) \tag{9}$$

Among i_t, f_t, O_t, C_t. They represent input information, forgotten information, output information and network status, ω indicates the weight parameter, b indicates the offset parameter, σ [•] indicates the sigmoid activation function. When building LSTM model, a large number of neural units and super parameters are introduced, which is easy to cause over-fitting phenomenon. In order to reduce the over-fitting phenomenon, the dropout technique was proposed. Therefore, this article uses dropout_ LSTM (Aykol et al., 2021) establishes a battery health prediction model.

In order to characterise the uncertainty of RUL prediction of battery remaining life and avoid the over-fitting phenomenon of the model, drop out_ MC is proposed to predict the remaining life. Bayes (Liu, 2021) variational inference is introduced to obtain the uncertainty of RUL prediction, while Bayes inference process is complex and the traditional neural network structure needs to be greatly improved, which makes the calculation of this method complex, thus limiting its application. Deshpande et al. (2012) proposed that the dropout neural network is approximately equivalent to the traditional neural network variational inference, while combining MC sampling technology to obtain the uncertainty of RUL prediction (Xiong et al., 2018). Based on the nonlinear mapping function, define a covariance function, namely

$$G(x,y)=\int p(\omega)p(b)\sigma\left(\omega^T x+b\right)\sigma\left(\omega^T y+b\right)d\omega db \tag{10}$$

Among $p(\omega)$ and $p(b)$ represent multidimensional normal distribution and one-dimensional normal distribution respectively; ω and b represents the weight matrix and offset. Use k the sub-MC sampling technique is used to obtain the finite rank covariance function, as shown in equation (10), where k indicates the second MC sampling.

$$\hat{G}(x,y)=\frac{1}{K}\sum\nolimits_{k=1}^{K}\sigma\left(\omega_k^T x+b_x\right)\left(\omega_k^T y+b_k\right) \tag{11}$$

about W_1, W_2, b. The approximate modelling based on Gauss mixed distribution is carried out, and the variational lower bound ELOB is obtained through MC sampling, namely

$$ELOB_{MC}=\sum\nolimits_{n=1}^{N}\lg\left[p(y_n\mid x_n,\hat{W}_1^n,\hat{W}_2^n,\hat{b}^n)\right]-KL[q\left(W_1,W_2,b\right)\|q\left(W_1,W_2,b\right) \tag{12}$$

where, KL [•] represents divergence, and represents multidimensional vector obtained by linear combination of multidimensional normal distribution and Bernoulli distribution. Then the lower bound of evidence (ELOB) is the same and the correlation distribution is as follows

$$ELOB_{MC}\propto-\frac{1}{N}\sum\nolimits_{n=1}^{N}\left\|y_n-\hat{y}_n\right\|_2^2-\frac{p_i}{\tau N}\left\|M_i\right\|_2^2-\frac{1}{\tau N}\|m\|_2^2 \tag{13}$$

where, represents the remaining life of the equipment, represents the regression value of the neural network model, N indicates the number of samples, τ is the model precision, probability p_i and matrix M_i as a matrix variation parameter. It can be seen from equation (13) that the approximate variational inference can be approximated by adding dropout to the neural network. For the specific derivation process and detailed parameter definition, refer to the published Xiong et al. (2018) such as Menglei et al. (2020). The framework of the proposed method is shown in Figure 2.

Figure 2 Dropout_ MC LSTM residual life prediction framework (see online version for colours)

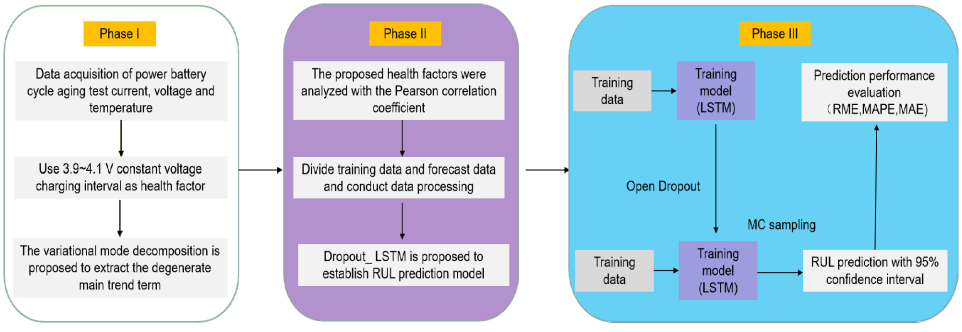

In this paper, 3.9~4.1 V constant voltage charging interval is used as the indirect health factor, and the effectiveness of the indirect health factor is verified by Spearson correlation analysis. This paper proposes dropout_ MC LSTM model to establish a health state prediction model (Qin et al., 2020). Through 1,000 times of MC sampling, the uncertainty characterisation of the residual life prediction results of lithium ion batteries was finally obtained and the 95% confidence interval was obtained. The high accuracy of the proposed model is verified by comparing the proposed method with the limit learning machine ELM and the nonlinear autoregressive neural network NARX of the existing methods.

2.3 Whale optimisation WOA-LSTM algorithm

WOA is a new swarm intelligence optimisation algorithm proposed by researchers such as Mirjalili Li (2019) of Griffith University in Australia in 2016. It is a meta-heuristic optimisation algorithm that simulates the predatory behaviour of humpback whales, and introduces the bubble net hunting strategy (Yan et al., 2022). In the WOA algorithm, humpback whales can accurately identify the position of prey and surround it. The position of each humpback whale can represent a feasible solution. The algorithm mainly includes three stages: encircling prey (Dai et al., 2019), bubble-net attacking and searching for prey (Zhang et al., 2019).

Where $p < 0.5$ and $|A| < 1$ to surround the prey, p is the random number generated in the range of [0, 1], A is the random number generated in the range of [0, 1], N, the position of each whale represents a feasible solution X. Humpback whales can identify the location of prey and surround it because the location of the optimal solution in the search space is not a priori known, so *WOA*. The algorithm assumes that the optimal whale individual position of the current population is the target prey or the nearest position to the target prey. After defining the optimal search location, other whale individuals will try to approach the optimal location of the current population, and the updated location formula is expressed as:

$$D = \left|CX^* - X(t)\right| \tag{14}$$

$$X(t+1) = X^*(t) - AD \tag{15}$$

where D is the distance between the current whale individual and the optimal position; T is the current iteration number; $X(t)$ is the position vector of the current whale individual; X^* is the current optimal solution position vector Where coefficient vector A, C The calculation formula is

$$A = 2ar - a \tag{16}$$

$$A = 2r \tag{17}$$

In equation (18): $a = 2 - \frac{2t}{t_{\max}}$, a linear reduction from 2 to 0; R is a random real number in [0, 1]; Is the maximum number of iterations.

$p \geq 0.5$, execute the bubble net attack hunting behaviour. When a whale is hunting, it will swim to its prey in a spiral motion. The mathematical formula for this behaviour is

$$X(t+1) = De^{bl}\cos(2\pi l) + X^*(t) \tag{18}$$

In equation (19): $D = |X^*–X(t)|$ Represents the distance between the current optimal whale individual position and prey; b is a constant used to define the shape of the helix; l is (–1, 1) a random number in the interval (Anselma et al., 2021). The whale adopts spiral mode, and needs to shrink the enclosure while swimming to the prey. Therefore, in the synchronous behaviour model, it is assumed that $1–P_i$ the probability of updating the position and existence of whales through the spiral model P_i the probability of the algorithm is to select the shrinking and enveloping mechanism. The mathematical model expression of the algorithm is

$$X(t+1) = \begin{cases} X^*(t) - ADp < P_i \\ De^{bl}\cos(2\pi l) + X^*(t), p \geq P_i \end{cases} \tag{19}$$

In equation (20): p is a random number of [0, 1], usually p = 05. When whales hunt, the closer they are to the prey, the smaller the value of a will be, and the smaller the value of A. In the iterative process of the algorithm, because the value of a is a vector that linearly decreases from 2 to 0, the value range of A is a random value of [a, – a]. When the value range of A is within [–1, 1], it means that the current position of the whale is anywhere between the original individual and the optimal individual, which indicates that the whale is approaching the optimal individual after the updated position. The algorithm sets that when $A < 1$, whales attack their prey.

When $p < 0$ 5 and $A > 1$, execute random search for prey. First, select a whale position randomly, update the position of other whales according to the selected position, force the whales to deviate from the prey, and then find a more suitable prey behaviour, which not only strengthens the exploration ability of the algorithm, but also enables the WOA algorithm to conduct global search. Its mathematical model expression is

$$D = \left|CX_{rand} - X\right| \tag{20}$$

$$X(t+1) = X_{rand} - AD \tag{21}$$

Among: X_{rand} Is the random position vector of individuals selected from the current population; $X(t + 1)$ is the position of the current whale in the $(t + 1)$ generation.

The parameter value of LSTM (Wang et al., 2019) model will have a great impact on the fitting ability of the model. Greff et al. studied the setting of LSTM-related parameters. The experimental results show that the number of hidden layer nodes and learning rate are the key parameters for the network setting, and the selection of the parameters is generally related to the characteristics of the data. Too large or too small will not necessarily achieve good prediction results. In order to find the optimal hyperparameters of the RUL prediction model for lithium batteries, WOA was used to optimise the three superparameters of LSTM, namely, the number of nodes L1, L2 and the learning rate Ir of LSTM (Somayaji et al., 2020) hidden layer. Take these three key parameters as the optimisation features, and use WOA algorithm to adjust and optimise the LSTM model to make the network structure model more match the data characteristics of lithium ion battery. In the hidden layer of LSTM, the output of each layer will be used as the input of the next layer, and finally the data will be output through the dense full connection layer (Chen and Lu, 2019). The algorithm steps of WOA-LSTM model are as follows:

Step 1 Data pre-processing. Firstly, the experimental data of lithium-ion battery is pre-processed, and the standardisation of data processing is the basis of modelling. Use the mapminmax function to map data to [–1, 1]. Secondly, the standardised experimental data is divided into training sets and test sets, and the experimental data is normalised.

Step 2 Initialise WOA algorithm parameters. Set the population number N, initialise the parameters (i.e., a, r, b, l, p), and randomly generate the position X according to the WOA.

Step 3 Determine the parameters and scope of optimisation in the LSTM network model, and take the number of nodes and learning rate of the two hidden layers in the network model as the object of optimisation.

Step 4 Calculate the individual fitness according to equation (7) and equation (8), save the optimal individual and the optimal position, and update A and C according to equation (9) and equation (10).

Step 5 generates a random number p, when $p \geq 0$ At 5, update the position according to equation (11); when $p < 0$ 5 and $A > 1$, update the position according to equation (14).

Step 6 Judge whether the conditions for terminating iteration are met. If the conditions for terminating iteration are met, the optimal value of the optimisation objective can be obtained; otherwise, return to step 2 to continue the operation until the termination condition is met.

Step 7 Reassign the optimised super parameters to the LSTM model, and train and predict through lithium battery data. The super parameters of LSTM neural network are optimised by WOA optimisation algorithm to minimise the MSE of the test set. The prediction block diagram of WOA-LSTM is shown in Figure 3.

Figure 3 WOA-LSTM model prediction flow chart

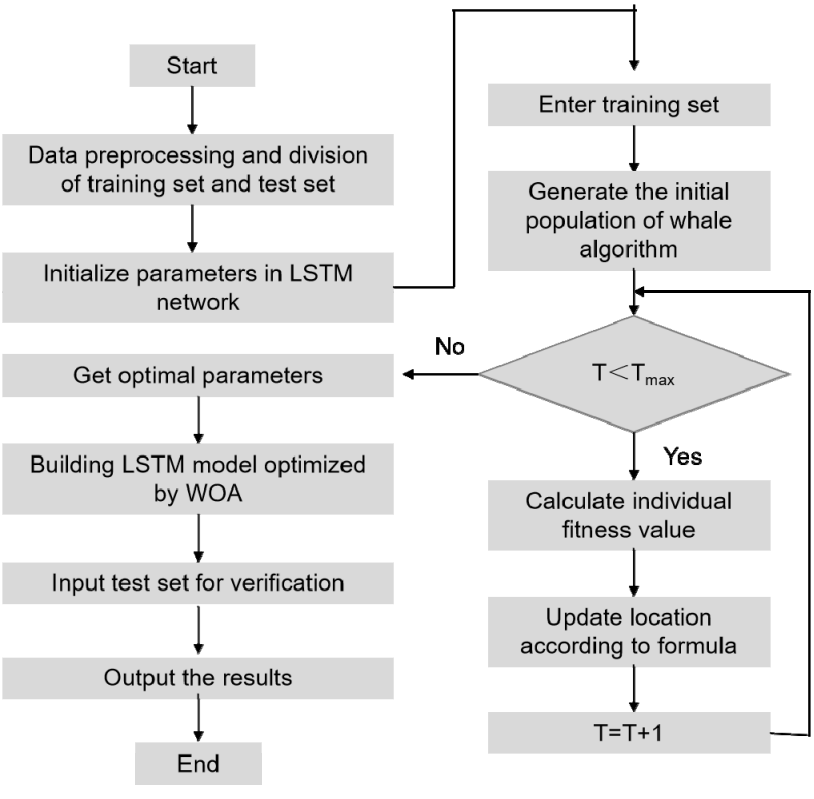

2.4 1D CNN-BiLSTM prediction model prediction

The prediction process of 1D CNN-BiLSTM model is shown in Figure 4. First, divide the lithium-ion battery capacity data into test sets and training sets according to different prediction points, and normalise the lithium-ion battery capacity data with MinMax (Zeng et al., 2019). Secondly, initialise various parameters of the model, then calculate and analyse the partial derivatives of the hidden layer, and finally obtain the prediction model of the remaining cycle life of the battery.

In this paper, NASA's 18650 model B0005 (B5) and B0006 (B6) lithium-ion battery dataset (Wang et al., 2017) is selected as the experimental data. The cycling charging and discharging process of NASA lithium-ion batteries is carried out in a constant temperature environment. 5. The capacity decline curve of B6 lithium-ion batteries is shown in Figure 5.

Figure 4 Prediction process of 1D CNN-BILSTM model (see online version for colours)

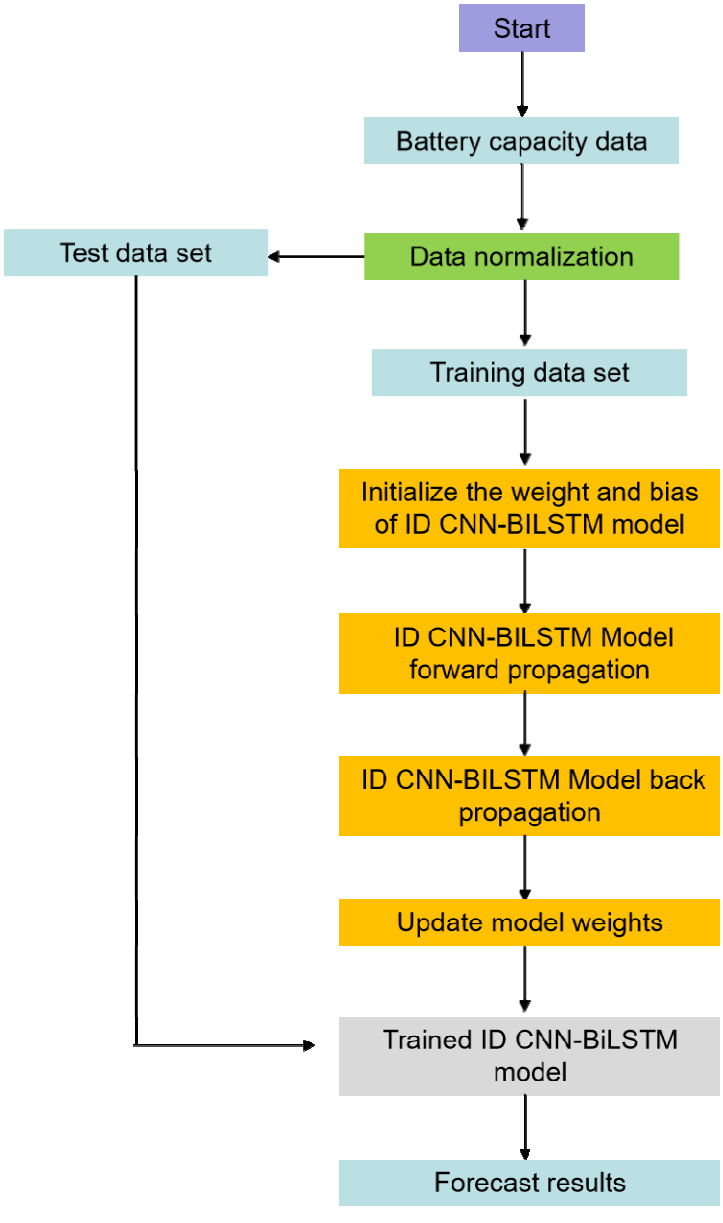

Figure 5 NASA lithium ion battery capacity decline curve (see online version for colours)

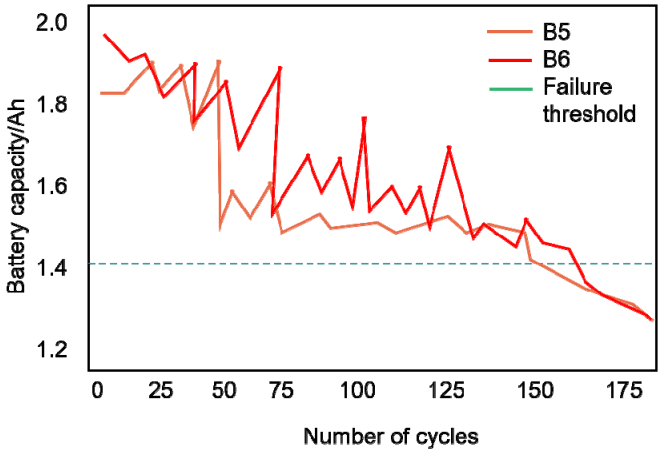

MinMax normalisation is performed on the capacity data of lithium-ion battery. MinMax normalisation formula can be defined as

$$x^* = \frac{x - \min(x)}{\max(x) - \min(x)} \tag{22}$$

where, x^* represents the normalised lithium ion battery capacity data, and x represents the lithium ion battery capacity data. In this paper, RUL absolute error (RULae), RMSE, MAE and coefficient of determination (r-square, R2) are used as the evaluation criteria of the prediction model. The definitions of RULae, RMSE, MAE and R2 are as follows:

$$RUL_{ae} = |LOP - EOL| \tag{23}$$

$$RMSE = \sqrt{\frac{1}{n}\sum_{i=1}^{n}(y_i - \hat{y}_i)^2} \tag{24}$$

$$MAE = \frac{1}{n}\sum_{i=1}^{n}\left|(y_i - \hat{y}_i)\right| \tag{25}$$

$$R^2 = 1 - \frac{\sum_i (\hat{y}_i - y_i)^2}{\sum_i (\bar{y}_i - y_i)^2} \tag{26}$$

Among y_i indicates the actual capacity data of lithium-ion battery, $\hat{y}_i$ represents the capacity value of lithium ion battery predicted by the model, represents the average of the actual data of lithium ion battery capacity. Life of prediction (LOP) of lithium-ion battery is the number of charge-discharge cycles when the SOH value of lithium-ion battery reaches the failure threshold for the first time.

3 Experiment

3.1 Battery experiment and data collection

The actual driving conditions of electric vehicles are complex and uncertain. In order to simulate the real driving conditions of electric vehicles as much as possible, the training data needs to be extended to other driving conditions. This paper uses the common dataset from the data warehouse of the centre for advanced life cycle engineering (CALCE) of the University of Maryland (Dufo-López et al., 2014). In the experiment, the A123 battery is placed in the temperature chamber for charging and discharging. The detailed parameters of the A123 battery are shown in Table 1, the measured current and voltage are shown in Figure 6, Figure 6(a), Figure 6(c) and Figure 6(e) are the measured current, and Figure 6(b), Figure 6(d) and Figure 6(f) are the measured voltage. The dynamic stress test (DST) dataset [Figures 6(a) and 5(b)] has different measurement results from the Federal Urban Driving Schedule (FUDS) dataset [Figures 6(c) and 6(d)) and US06 dataset [Figures 6(e) and 6(f)]. DST, FUDS and US06 have obvious differences in discharge current and voltage. Because the training data is often more than the test data, this paper uses DST and FUDS dataset as the training dataset, US06 as the test dataset, and the temperature is 10°C, 20°C, 30°C and 40°C.

Table 1 A123 battery parameters

Parameters	*Value (composition)*
Rated capacity/(A·h)	2.230
chemical composition	LiFePO4
Weight/g	76
Size/mm	25.4
Length/mm	65

In order to verify whether the GRU model is applicable to the SOC estimation of lithium ion batteries, the simulation results of RNN model and LSTM model are compared and analysed. The network model structure and parameters are unified as the data given in Table 2. First of all, it is necessary to determine the number of iterations. In this paper, the number of iterations is selected under normal temperature of 20°C. Table 3 and Figure 6 show the relationship between the number of iterations and the error of the SOC estimation of three kinds of cyclic neural networks for lithium-ion batteries.

It can be seen from Table 3 that at the beginning of the 10 iterations, RNN has a high accuracy, and the relative error of LSTM and GRU is relatively large, which is related to the random initialisation parameters of the network. RNN initialisation parameters are closer to the optimal parameters. When the number of iterations reaches 20, the accuracy of LSTM and GRU two variants of the cyclic network is higher than that of the traditional RNN. RNN reaches the optimum value near the iteration number of 50. However, with the increase of the iteration number, the model error increases due to over-fitting, so the number of iterations of RNN model experiment should not be too much. The error of LSTM and GRU continues to decrease as the number of iterations increases. However, the required error is a training error and cannot reflect the actual test error. When the training error is far less than 0.05% of the test accuracy of the battery test instrument, the noise of the battery test instrument will be over-fitted. It can be seen from

Figure 7 that the three algorithms converge to a higher accuracy when the number of iterations is 50; the iterative MSE relationship is GRU < LSTM < RNN; the error is around 0.05% when the number of iterations is 100. Therefore, in order to prevent over-fitting, the number of iterations in the subsequent experiments of this paper is fixed at 100.

Figure 6 Waveform of measured current and measured voltage (a) DST dataset measured current (b) DST dataset measured current voltage (c) FUDS dataset measured current (d) FUDS dataset measured current voltage (e) US06 dataset measured current (f) US06 dataset measured current voltage (see online version for colours)

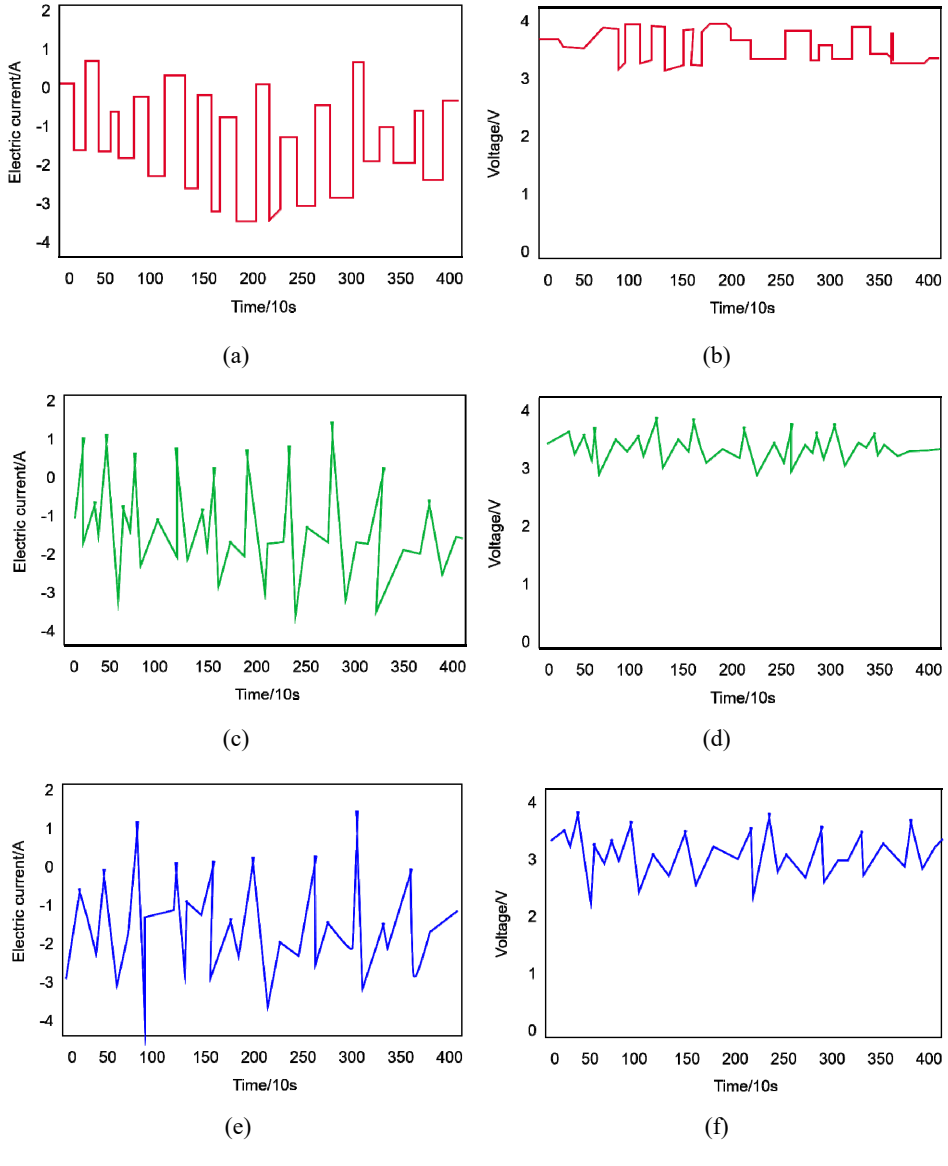

Figure 7 The relationship between the number of iterations and MSE (see online version for colours)

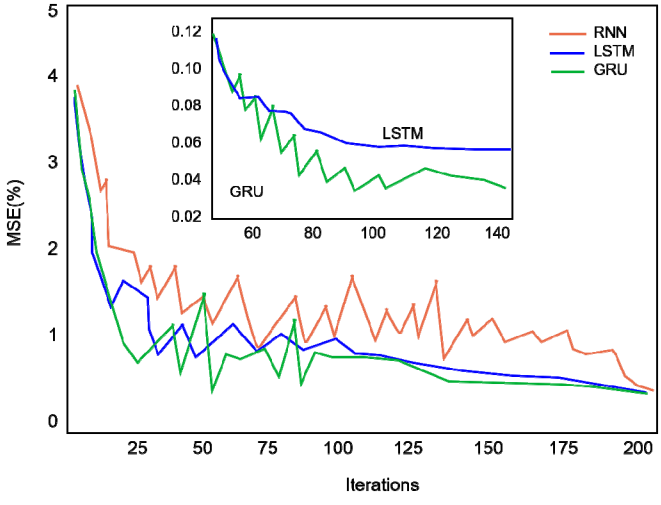

Table 2 Network model structure and parameters

Structure and parameters	*Value and name*
Sampling time/s	5
time step	30
Training batch size	3,000
Number of hidden layers	2
Number of hidden layer nodes	32
Activation function	ReLU
Training optimisation algorithm	Adma
Initial learning rate	0.01
Optimisation objective function	MSE

Table 3 The relationship between the number of iterations and the error

Iterations	*Training MSE (%)*		
	RNN	*LSTM*	*GRU*
10	2.068 4	3.726 3	3.117 6
20	2.203 1	1.280 7	1.079 9
30	0.577 3	0.230 0	0.787 5
40	0.343 9	0.192 3	0.204 7
50	0.220 8	0.108 1	0.121 8
100	0.538 8	0.044 0	0.026 6
200	0.218 6	0.029 9	0.010 3
300	8.630 7	0.016 5	0.004 1
Average time per iteration/s	0.3866	1.2818	0.9768

Table 4 shows the SOC estimation error of GRU model lithium-ion battery at different temperatures, with MAE of 1.905%, MSE of 0.065% and RMSE of 2.508%. MAE has met within 2% of the estimated demand of many SOC. The estimated results of SOC at different temperatures of lithium ion battery in GRU model are shown in Figure 8. The estimated error value fluctuates slightly and the frequency of fluctuation is gentle. The estimated fluctuation trend is similar to that in Figure 5.

Table 4 GRU model lithium-ion battery SOC estimation error at different temperatures

Temperature	*MAE (%)*	*MSE (%)*	*RMSE (%)*
10°C	1.738 8	0.048 7	2.207 2
20°C	1.608 2	0.049 8	2.232 2
30°C	1.719 6	0.048 3	2.197 8
40°C	2.555 3	0.115 3	3.396 6
Average	1.905 2	0.064 5	2.507 5

Figure 8 SOC estimation results of lithium ion battery at different temperatures in GRU model (a) 10°C (b) 20°C (c) 30°C and (d) 40°C (see online version for colours)

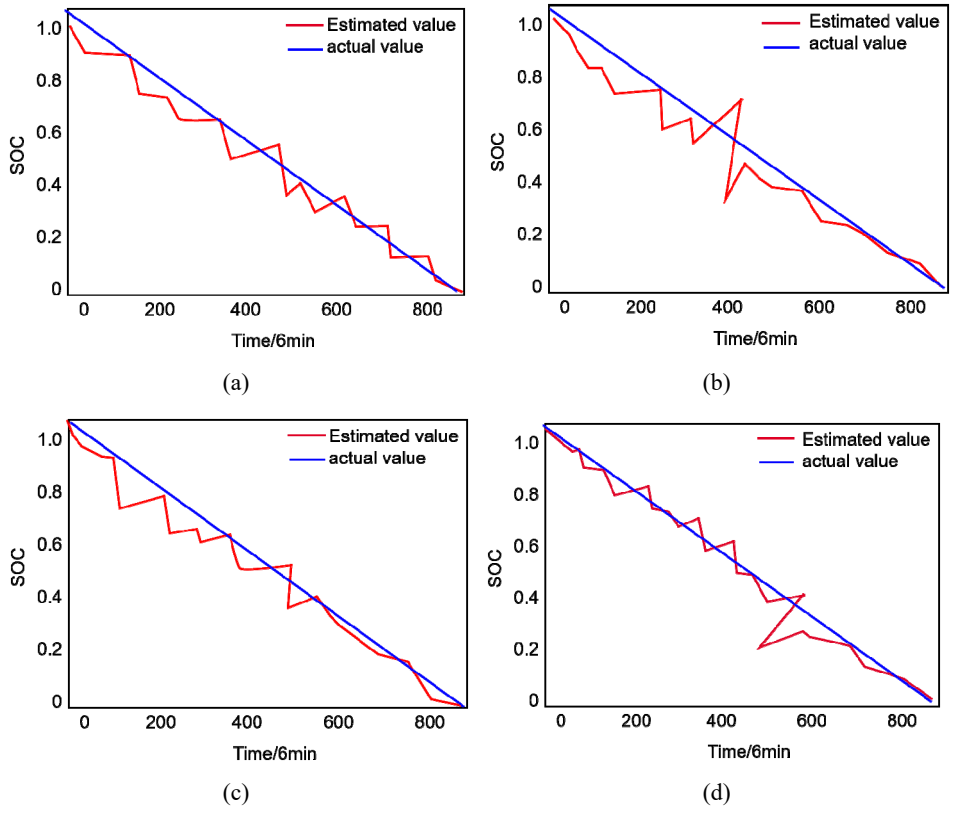

3.2 Analysis of experimental results

Using the failure data of B05 and B06 batteries in the NASA public dataset for experimental simulation, the data of health factors in Table 5 is used as the input variable of the model, and the residual capacity of lithium ion batteries is used as the output variable of the model, so as to build a fitting model between the extracted health factors and the actual capacity of the battery (Menglei et al., 2020). The cycle charge and discharge cycle of lithium battery is 168, so 50% of the total dataset of lithium battery is used as training data to input the neural network model, and the remaining 50% is used as the test set to verify the model. In the B05 battery experiment, the optimal hyperparameters of the WOA-LSTM model are set as follows: the number of cells in the first hidden layer is 12, the number of cells in the second hidden layer is 16, and the learning rate is 0 003 9; The optimal hyperparameter settings obtained in the B06 battery experiment are: the number of cells in the first hidden layer is 10, the number of cells in the second hidden layer is 20, and the learning rate is 0 005 8. The optimal hyperparameters obtained after optimisation are reassigned to LSTM neural network, and the network prediction model is constructed again.

Table 5 Indirect influence factors of lithium battery performance degradation

Serial number	*Indirect influence factor*	*Indicator name*
1	F1	Equal-pressure rise charging interval
2	F2	Constant current drop charging time interval
3	F3	Constant voltage drop discharge time interval
4	F4	Average temperature during charging
5	F5	Average temperature during discharge

Figure 9 WOA fitness curve (a) B05 battery and (b) B06 battery (see online version for colours)

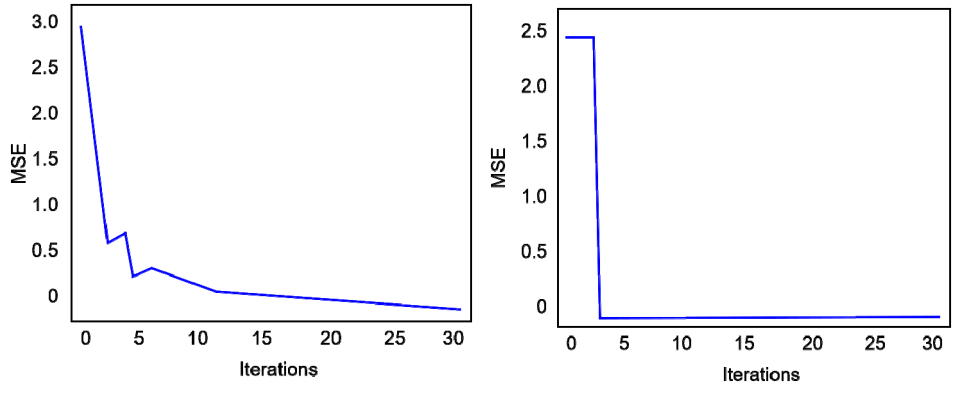

(a) (b)

PSO is a commonly used parameter optimisation algorithm, but the main advantage of the selected WOA compared with PSO is that WOA uses random or optimal search agents to simulate hunting behaviour, and the search path is theoretically visible and controllable, the algorithm operation and implementation process is relatively simple, the parameters to be adjusted are few, and the ability to jump out of local optimisation is

strong. Elman is a kind of feedforward neural network with local memory function and local feedback connection, and is a relatively common regression prediction model. Therefore, the standard LSTM algorithm, Elman algorithm, PSOLSTM algorithm and WOA-LSTM algorithm are used to simulate the constructed prediction model and compare the error of the prediction results. Figure 9 shows the fitness curve of the WOA optimisation algorithm. The maximum number of iterations is set to 30. Taking MSE as the evaluation index, it can be seen intuitively that B05 battery is stable in the 12th iteration; B06 battery reached a stable state at the fourth iteration.

As shown in Figure 10, the capacity prediction result curves of the four algorithms for B05 and B06 batteries are shown. From Figure 10(a) and Figure 10(b), it can be seen that the prediction results of the LSTM network model optimised by WOA are significantly closer to the actual battery capacity value, so the prediction performance of WOA-LSTM algorithm is significantly better than PSO-LSTM algorithm, Elman algorithm and standard LSTM algorithm. This also shows that the prediction accuracy of the model can be greatly improved by using the WOA to optimise the parameters of LSTM.

Figure 10 Error comparison chart (a) B05 battery and (b) B06 battery (see online version for colours)

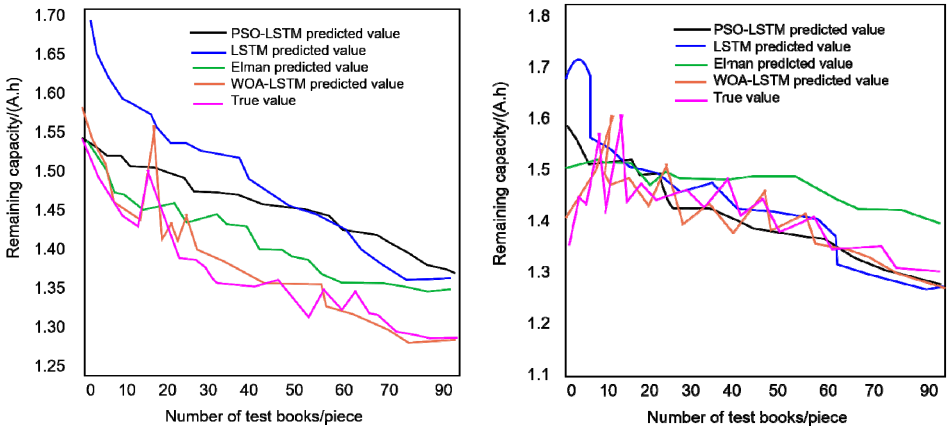

(a) (b)

Table 6 shows the specific prediction error values of each index. The closer the error is to 0, the higher the prediction accuracy and the better the model. Among them, the MAE index of B05 battery decreased the most significantly, which was 7. 5% lower than that of LSTM 68%, 3. 5% lower than Elman 24%, 4% lower than PSO-LSTM 02%; RMSE index decreased significantly, 7. 7% lower than LSTM 39%, 3. 5% lower than Elman 04%, 3. 5% lower than PSO-LSTM 83%; compared with LSTM, MAPE index also decreased by 5. 5% 57%, 3. 5% lower than Elman 68%, 2. 5% lower than PSO-LSTM 95%. Similarly, it can be seen from Table 6 that the MAE index of B06 battery is the most significantly reduced, which is 10% lower than that of LSTM 16%, 4. 5% lower than Elman 44%, 3. 5% lower than PSO-LSTM 88%; The RMSE index decreased significantly, which was 9. 9% lower than that of LSTM 49%, 3. 5% lower than Elman 49%, 3. 5% lower than PSO-LSTM 08%; Compared with LSTM, MAPE index also decreased by 7. 7% 78%, 4. 5% lower than Elman 24%, 3. 5% lower than PSO-LSTM 85%.

Table 6 Comparison of experimental results of various algorithms

Battery	*Evaluating indicator*	*LSTM*	*Elman*	*PSO-LSTM*	*WOA-LSTM*
B05	MAE	0. 133 1	0. 088 7	0. 096 5	0. 056 3
	RMSE	0. 144 9	0. 101 4	0. 109 3	0. 071 0
	MAPE	0. 097 2	0. 078 3	0. 071 0	0. 041 5
B06	MAE	0. 159 9	0. 102 7	0. 097 1	0. 058 3
	RMSE	0. 178 0	0. 118 0	0. 083 9	0. 083 1
	MAPE	0. 123 2	0. 087 9	0. 083 9	0. 045 5

Figure 11 shows the error comparison histogram of the four algorithms. Using MAE, RMSE, and MAPE to analyse the error results, we can intuitively see the prediction performance of the four algorithms. Among them, the LSTM algorithm has larger indicators, followed by Elman algorithm, PSO-LSTM algorithm with smaller errors, and WOA-LSTM algorithm has smaller errors than the other three algorithms.

Figure 11 Error comparison of various indicators (a) B05 battery (b) B06 battery (see online version for colours)

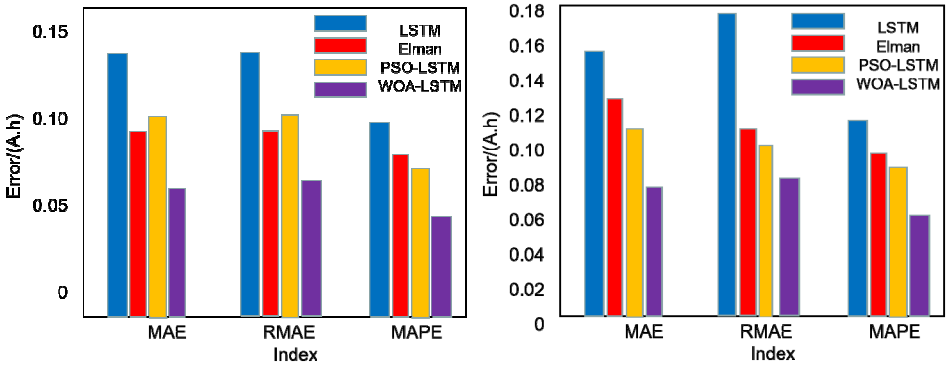

(a) (b)

4 Conclusions

In order to improve the accuracy of residual life (RUL) prediction and obtain the uncertainty representation of RUL prediction, this paper proposes a LSTM method based on drop out Monte Carlo to predict battery health. In this method, the time interval of constant voltage charging is selected as the indirect health factor. At the same time, the variational mode decomposition (VMD) is proposed to obtain the battery degradation trend item, effectively reducing the capacity regeneration and random interference phenomenon in the battery use process, and LSTM is established to improve the RUL prediction accuracy. This paper proposes a drop out Monte Carlo sampling method to obtain the uncertainty representation of RUL., Finally, two FNN networks, two CNN networks, one LSTM network and SCN are used for comparative experiments. The method in this paper is to estimate the SOC at different temperatures. In practical application scenarios, the battery temperature is dynamic, so there is no discussion on the

system temperature change and aging adaptability. The decomposition process of the measured current signal is an empirical process, and it is not easy to quickly estimate the SOC of the battery.

References

Angenendt, G., Zurmühlen, S., Mir-Montazeri, R. et al. (2016) 'Enhancing battery lifetime in PV battery home storage system using forecast based operating strategies', *Energy Procedia*, Vol. 99, No. 2, pp.80–88.

Anselma, P.G., Kollmeyer, P., Lempert, J. et al. (2021) 'Battery state-of-health sensitive energy management of hybrid electric vehicles: lifetime prediction and ageing experimental validation', *Applied Energy*, Vol. 285, No. 5, p.116440.

Aykol, M., Gopal, C.B., Anapolsky, A. et al. (2021) 'Perspective – combining physics and machine learning to predict battery lifetime', *Journal of The Electrochemical Society*, Vol. 168, No. 3, p.30525.

Chen, J. and Lu, X. (2019) 'Analysis of the impact of monomer inconsistency on the battery life of new energy passenger cars', *Times Agricultural Machinery*, Vol. 46, No. 10, pp.35–36.

Dai, H., Zhang, Y., Wei, X. and Jiang, B. (2019) 'Research on residual life prediction of lithium ion batteries', *Power Technology*, Vol. 43, No. 12, pp.2029–2035.

Deshpande, R., Verbrugge, M., Cheng, Y.T. et al. (2012) 'Battery cycle life prediction with coupled chemical degradation and fatigue mechanics', *Journal of the Electrochemical Society*, Vol. 159, No. 10, p.A1730.

Duan, Y. (2021) *Life Test and Health State Estimation of Lithium-Ion Battery*, Zhejiang University.

Dufo-López, R., Lujano-Rojas, J.M. and Bernal-Agustín, J.L. (2014) 'Comparison of different lead–acid battery lifetime prediction models for use in simulation of stand-alone photovoltaic systems', *Applied Energy*, Vol. 115, No. 3, pp.242–253.

Li, D. (2019) 'Evaluation method for battery life of TIA mobile terminal products', *Safety and Electromagnetic Compatibility*, Vol. 2019, No. 6, pp.71–75.

Liao, L. and Köttig, F. (2014) 'Review of hybrid prognostics approaches for remaining useful life prediction of engineered systems, and an application to battery life prediction', *IEEE Transactions on Reliability*, Vol. 63, No. 1, pp.191–207.

Liu, Q. (2021) *Research on Optimization Control Strategy of Electric Vehicle Acceleration Process for Energy Consumption and Battery Life*, South China University of Technology.

Lv, Q., Liu, C., He, W. and Jin, H. (2022) 'Life prediction method of power battery based on SVM and decision tree', *Electrotechnical*, Vol. 2022, No. 20, pp.36–38.

Mansouri, S.S., Karvelis, P., Georgoulas, G. et al. (2017) 'Remaining useful battery life prediction for UAVs based on machine learning', *IFAC-PapersOnLine*, Vol. 50, No. 1, pp.4727–4732.

Menglei, S., Li, J., Zhao, M., Zhang, M., Shao, G. and Wang, Z. (2020) 'Research progress in lithium ion battery life prediction', *Battery Industry*, Vol. 24, No. 5, pp.255–263.

Muenzel, V., de Hoog, J., Brazil, M. et al. (2015) 'A multi-factor battery cycle life prediction methodology for optimal battery management', *Proceedings of the 2015 ACM Sixth International Conference on Future Energy Systems*, pp.57–66.

Ou, H., Huang, D., Lin, K., Wang, Y., Mo, Z., Li, J. and Niu, J. (2021) 'Study on battery life prediction mechanism and feasibility of implantable cardiac pacemaker based on discharge characteristics', *Chinese Journal of Cardiac Pacing and Electrophysiology*, Vol. 35, No. 6, pp.573–576, DOI: 10.13333/j.cnki.cjcpe.2021.06.013.

Qin, D., Zhang, X. and Yao, M. (2020) 'Optimization of PHEV energy management strategy considering energy consumption economy and battery life', *Journal of Chongqing University*, Vol. 43, No. 10, pp.1–11.

Shen, D., Xu, T., Wu, L. et al. (2019) 'Research on degradation modeling and life prediction method of lithium-ion battery in dynamic environment', *IEEE Access*, Vol. 7, No. 4, pp.130638–130649.

Somayaji, S.R.K., Alazab, M., Manoj, M.K. et al. (2020) 'A framework for prediction and storage of battery life in IoT devices using DNN and blockchain', *2020 IEEE Globecom. Workshops* (GC Wkshps. IEEE, pp.1–6.

Sulzer, V., Mohtat, P., Aitio, A. et al. (2021) 'The challenge and opportunity of battery lifetime prediction from field data', *Joule*, Vol. 5, No. 8, pp.1934–1955.

Wang, D., Yang, F., Zhao, Y. et al. (2017) 'Battery remaining useful life prediction at different discharge rates', *Microelectronics Reliability*, Vol. 78, No. 7, pp.212–219.

Wang, G. and Di, X. (2022) 'Research on an online life prediction method of lithium battery based on PCA and correlation vector machine', *Journal of Liaoning University of Petroleum and Chemical Technology*, Vol. 42, No. 6, pp.84–89.

Wang, M. (2021) *Research on Residual Life Prediction Method of Lithium Ion Battery Based on Machine Learning*, Anhui University of Technology, DOI: 10.26918/d.cnki.ghngc.2021.00635.

Wang, N., Liu, Y., Jiang, K. and Chen, Z. (2019) 'Life prediction of lithium iron phosphate battery based on VPSO-SVM', *Journal of Chongqing University of Technology* (Natural Science), Vol. 33, No. 11, pp.173–177+230.

Xiong, R., Zhang, Y., Wang, J. et al. (2018) 'Lithium-ion battery health prognosis based on a real battery management system used in electric vehicles', *IEEE Transactions on Vehicular Technology*, Vol. 68, No. 5, pp.4110–4121.

Yan, L., Peng, J., Gao, D. et al. (2022) 'A hybrid method with cascaded structure for early-stage remaining useful life prediction of lithium-ion battery', *Energy*, Vol. 243, No. 5, p.123038.

Yang, Y. (2021) 'A machine-learning prediction method of lithium-ion battery life based on charge process for different applications', *Applied Energy*, Vol. 292, No. 2, p.116897.

Yu, L., Wu, Z., Jiang, Q. and Xiong, S. (2022) 'Life prediction of proton exchange membrane fuel cells based on machine learning', *Modern Machinery*, Vol. 2022, No. 5, pp.1–5.

Zeng, X., Wang, X., Song, D., Yang, N. and Wang, Z. (2019) 'Energy management optimization of plug-in hybrid electric vehicles considering battery life', *Journal of Zhejiang University* (Engineering Edition), Vol. 53, No. 11, pp.2206–2214.

Zhang, F., Fang, L., Lu, C., Deng, H., Zhou, Z. and Ma, J. (2021) 'Analysis of the benefits of energy storage taking into account battery life in the FM market', *Zhejiang Electric Power*, Vol. 40, No. 12, pp.61–68, DOI: 10.19585/j.zjdl.202112008.

Zhang, M., Feng, Y., Peng, X., Lu, L., Wang, W. and Xu, X. (2019) 'Research on automobile power battery life test based on working conditions', *Neijiang Science and Technology*, Vol. 40, No. 11, pp.32–33.

Zhang, N., Liu, Y., Tang, J. and Li, J. (2022) 'Prediction method of battery cycle life based on KF-BPNN fusion algorithm', *Journal of Naval Engineering University*, Vol. 34, No. 5, pp.39–40.

Zhu, H., Lv, Z., Di, R., Sun, X. and Hao, K. (2022) 'Improved neural network lithium battery life prediction simulation of MD-MTD', *Journal of Xi'an University of Technology*, Vol. 42, No. 6, pp.620–626.

Zong, L., Zhu, F., Du, F. and Wang, C. (2022) 'Analysis of factors affecting the life decay of electric vehicle power battery', *Power Technology*, Vol. 46, No. 12, pp.1353–1356